Equilibration protocol. After 200 steps of conjugate gradient minimization on the water molecules, 50 ps of solvent equilibration at 298 K were calculated with ions free and protein/RNA fixed except for hydrogens. Followed a restart at 10 K and heating to 298 K in steps of 50 K, with 10 ps of simulation at each temperature without applying any constraints. For the simulations at low-salt conditions, the productive MD phase followed immediately. For simulations at 1 M NaCl, additional heating was performed to obtain a rapid redistribution of the ions. Therefore, the system was simulated at 900 K for 5 ps, followed by cooling to 298 K over 2 ps, with protein and RNA kept fixed in both phases.

Following equilibration, one reference trajectory of 1.75 ns at low-salt conditions and two independent trajectories of 1.55 ns and 1.10 ns, with slight differences in the heating phase, were calculated for the high-salt system. The results reported for the 1 M NaCl conditions were reproducibly observed in both high-salt trajectories.

Acknowlegments

T.H. was supported by an EMBO long-term fellowship and a DFG grant. E.W. thanks the Institut Universitaire de France for supporting grants.

Correspondence should be addressed to E.W. *email: westhof@ibmc.u-strasbg.fr*

Received 7 January, 1999; accepted 25 March, 1999.

1. Nagai, K. & Mattaj, I.W. *RNA–protein interactions*. (IRL Press, Oxford; 1994).
2. Anderson, C.F. & Record, M.T. *Annu. Rev. Phys. Chem.* **46**, 657–700 (1995).
3. Record, M.T., Zhang, W. & Anderson, C.F. *Adv. Prot. Chem.* **51**, 281–353 (1998).
4. Steitz, J.A., Black, D.L., Gerke, V., Parker, K.A., Krämer, A. *et al.* In *Structure and function of major and minor small nuclear ribonucleoprotein particles* (ed. Birnstiel, M.L.) 115–154 (Springer-Verlag, New York; 1988).
5. Nagai, K., Oubridge, C., Ito, N., Avis, J. & Evans, P.R. *Trends Biochem. Sci.* **20**, 235–240 (1995).
6. Scherly, D., Boelens, W., Van Venrooij, W.J., Dathan, N.A., Hamm, J. *et al. EMBO J.* **8**, 4163–4170 (1989).
7. Hall, K.B. & Stump, W.T. *Nucleic Acids Res.* **20**, 4283–4290 (1992).
8. Oubridge, C., Ito, N., Evans, P.R., Teo, C.-H. & Nagai, K. *Nature* **372**, 432–438 (1994).
9. Manning, G.S. *J. Chem. Phys.* **51**, 924–933 (1969).
10. Braunlin, W.H. *Adv. Biophys. Chem.* **15**, 89–139 (1995).
11. Nagai, K., Oubridge, C., Jessen, T.H., Li, J. & Evans, P.R. *Nature* **348**, 515–520 (1990).
12. Allain, F.H.-T., Gubser, C.C., Howe, P.W.A., Nagai, K., Neuhaus, D. *et al. Nature* **380**, 646–650 (1996).
13. van Gelder, C.W.G., Gunderson, S.I., Jansen, E.J.R., Boelens, W.C., Polycarpou-Schwarz, M. *et al. EMBO J.* **12**, 5191–5200 (1993).
14. Ibragimova, G.T. & Wade, R.C. *Biophys. J.* **74**, 2906–2911 (1998).
15. Pearson, N.D. & Prescott, C.D. *Chem. Biol.* **4**, 409–414 (1997)
16. Hermann, T. & Westhof, E. *Curr. Opin. Biotechnol.* **9**, 66–73 (1998).
17. Pearlman, D.A., Case, D.A., Caldwell, J.W., Ross, W.S., Cheatham, T.E. *et al. AMBER 4.1* (San Francisco, California; 1994).
18. Cornell, W.D., Cieplak, P., Bayly, C.I., Gould, I.R., Merz, K.M. *et al. J. Am. Chem. Soc.* **117**, 5179–5197 (1995).
19. Ryckaert, J.P., Ciccotti, G. & Berendsen, H.J.C. *J. Comput. Phys.* **23**, 327–336 (1977).
20. Berendsen, H.J.C., Postma, J.P.M., van Gunsteren, W.F., Dinola, A. & Haak, J.R. *J. Chem. Phys.* **81**, 3684–3690 (1984).
21. Darden, T.A., York, D. & Pedersen, L.G. *J. Chem. Phys.* **98**, 10089–10092 (1993).
22. Berendsen, H.J.C., Grigera, J.R. & Straatsma, T.P. *J. Phys. Chem.* **97**, 6269–6271 (1987).
23. Auffinger, P. & Beveridge, D.L. *Chem. Phys. Lett.* **234**, 413–415 (1995).
24. Dang, L.X., Pettitt, B.M. & Rossky, P.J. *J. Chem. Phys.* **96**, 4046–4047 (1992).

Stability of hairpin ribozyme tertiary structure is governed by the interdomain junction

Nils G. Walter[1], John M. Burke[1] and David P. Millar[2]

[1]Markey Center for Molecular Genetics, Department of Microbiology and Molecular Genetics, The University of Vermont, Burlington, Vermont 05405, USA. [2]Department of Molecular Biology (MB-19), The Scripps Research Institute, 10550 North Torrey Pines Road, La Jolla, California 92039, USA.

The equilibrium distributions of hairpin ribozyme conformational isomers have been examined by time-resolved fluorescence resonance energy transfer. Ribozymes partition between active (docked) and inactive (extended) conformers, characterized by unique interdomain distance distributions, which define differences in folding free energy. The active tertiary structure is stabilized both by specific interactions between the catalytic and the substrate-binding domains and by the structure of the intervening helical junction. Under physiological conditions, the docking equilibrium of the natural four-way junction dramatically favors the active conformer, while those of a three-way and the two-way junction used in gene therapy applications favor the inactive conformer.

The discovery of ribozymes[1,2] opened up new avenues for understanding structure-function relationships in RNA, since catalytic function reports the presence of an active tertiary structure. Recent advances in NMR spectroscopy and X-ray crystallography have revealed atomic details of RNA structure[3] but are largely unable to report conformational changes that are essential for biological function. Lower resolution methods such as fluorescence quenching assays[4], cross-linking studies[5], absorbance spectroscopy[6], electrophoretic mobility[7], hydroxyl radical footprinting[8], and differential probe hybridization[9] have recently begun to illuminate the complexity of RNA tertiary structure folding pathways.

A model system that is useful for studying RNA folding is the hairpin ribozyme, a reversible endoribonuclease that catalyzes cleavage and ligation reactions necessary for the rolling circle replication of a family of satellite RNAs associated with plant viruses[10]. Their proliferation involves autolysis of the replicated concatamer by a site-specific 2'-OH nucleophilic attack, and cyclization of the resulting RNA monomers. In the negative strand of tobacco ringspot virus satellite ((-)-sTRSV) RNA, the hairpin ribozyme is embedded within a four-way helical junction[11]. For biochemical studies *in vitro*, a minimal *trans*-acting ribozyme was engineered by deleting two of the four junction arms[11] (Fig. 1*a*). The resulting construct, containing a two-way junction, has been used for targeted RNA inactivation within mammalian cells, and is the basis for experimental strategies in human gene therapy of genetic and viral diseases[12].

No high-resolution data on the tertiary structure of the hairpin ribozyme are yet available[13]. Previous evidence has shown that catalytic activity requires a sharp bend about the hinge of the junction between the two domains A and B of the ribozyme–substrate complex (Fig. 1*a*), enabling a specific interdomain docking interaction[13]. Pre-steady state analysis has revealed biphasic kinetic behavior that results from formation of an alternative conformer of the ribozyme–substrate complex[14]; the two domains adopt an extended structure that lacks catalytic activity but can reversibly bind substrate[15]. Steady-

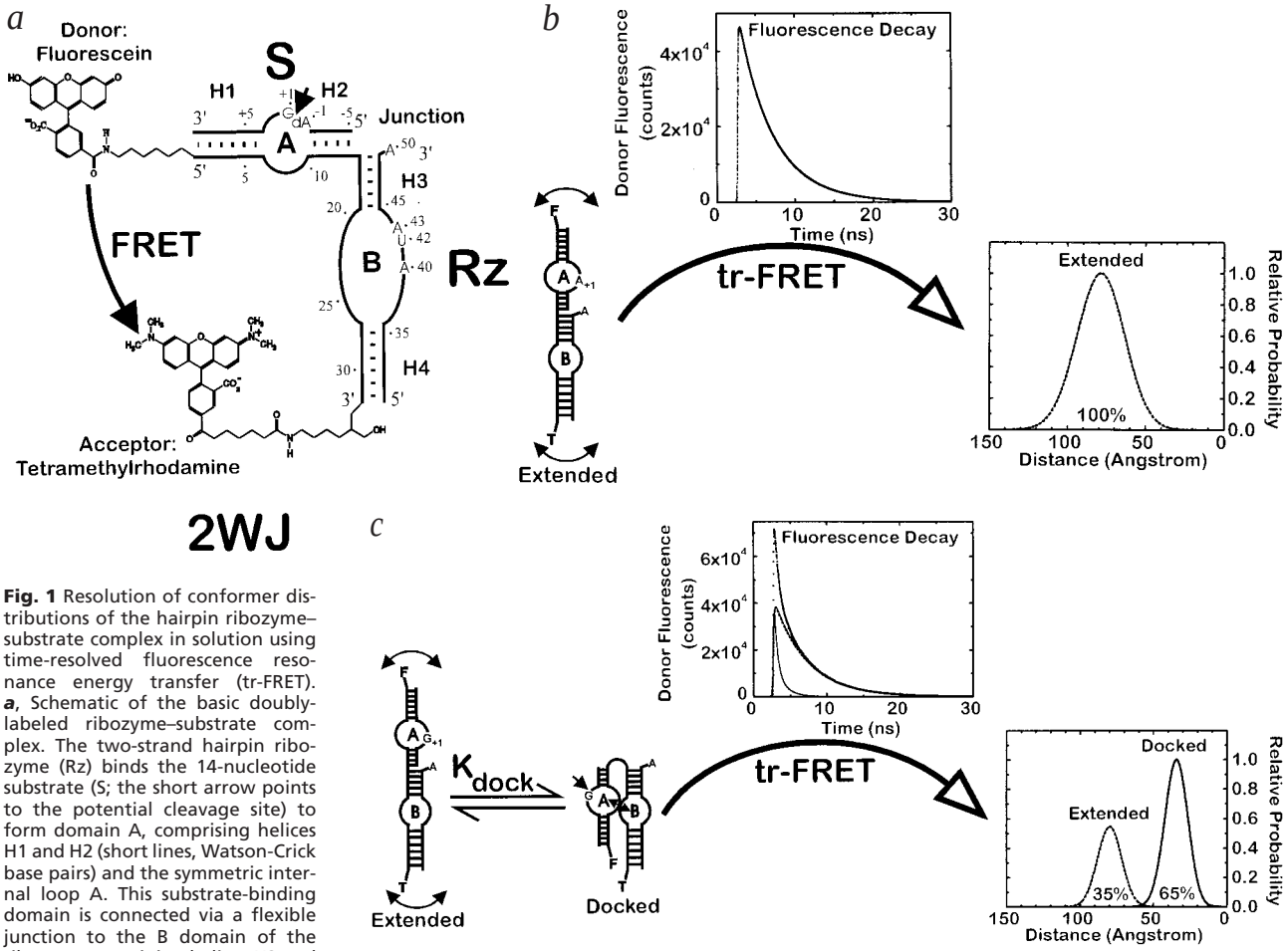

Fig. 1 Resolution of conformer distributions of the hairpin ribozyme–substrate complex in solution using time-resolved fluorescence resonance energy transfer (tr-FRET). ***a***, Schematic of the basic doubly-labeled ribozyme–substrate complex. The two-strand hairpin ribozyme (Rz) binds the 14-nucleotide substrate (S; the short arrow points to the potential cleavage site) to form domain A, comprising helices H1 and H2 (short lines, Watson-Crick base pairs) and the symmetric internal loop A. This substrate-binding domain is connected via a flexible junction to the B domain of the ribozyme containing helices H3 and H4 and an asymmetric internal loop B. We refer to this design as a two-way junction (2WJ). Fluorescein (F) and tetramethylrhodamine (T) are coupled as donor and acceptor pair to opposite ends of the complex to enable distance-dependent FRET (curved arrow). Cleavage is blocked by a 2′-deoxy modification of the attacking nucleophile of the ribose of A_{-1}. ***b***, Revealing a single conformer by tr-FRET. A G+1→A mutant substrate impairs docking of the ribozyme–substrate complex and results in a flexible extended conformer with F and T at distant ends. The time-resolved donor (F) emission decay of this complex under standard conditions (50 mM Tris-HCl, pH 7.5, 12 mM $MgCl_2$, at 17.8 °C) is measured and the donor–acceptor distance information extracted. We found that a single continuous, three-dimensional Gaussian distance distribution (dashed line) fits the data very closely (giving a reduced χ^2 of 1.08). ***c***, Revealing an equilibrium between two conformers by tr-FRET. If the complex can fold from the initial extended structure into the docked conformer (in the presence of a G+1 base) the donor decay data (dots) can only be fitted with the sum of two Gaussian distance distributions (χ^2 = 1.28), revealing the presence of both extended and docked conformers (deconvoluted contributions to the donor decay represented by solid and dashed lines, respectively). The relative abundance of these isomers is obtained directly from the analysis and is reflected in the relative heights of the corresponding distance distributions. Thus, tr-FRET defines the equilibrium constant K_{dock} (from the ratio docked fraction/extended fraction) between docked and extended conformers. Note that a 3′ dangling adenosine on the ribozyme near the hinge favors docking of the complex (Table 1).

state fluorescence resonance energy transfer (FRET) has shown that an undocked conformer is a folding intermediate in the reaction pathway, preceding docking and cleavage, and has allowed us to elucidate docking rates and requirements[16]. Strikingly, the predominant mechanism of inhibition by mutations and functional group substitutions (for example, a G+1→A mutation, where +1 refers to the nucleotide immediately 3' of the cleavage site) is interference with docking of the two domains[16,17]. Steady-state FRET is, however, unable to observe the equilibrium distribution between alternative conformers of a nucleic acid structure and instead reports an average measurement from all conformers present[16,18–20].

Time-resolved fluorescence resonance energy transfer (tr-FRET) permits the spectroscopic resolution of the two intrinsic conformers of hairpin ribozyme–substrate complexes in solution, by examining the influence of an acceptor fluorophore (tetramethylrhodamine) on the fluorescence lifetime of a donor fluorophore (fluorescein) (Fig. 1). tr-FRET analysis quantifies the equilibrium position between the alternative structural isomers under physiological conditions and provides donor-acceptor distance information with near Å resolution, by fitting life-time data with theoretical energy transfer functions for one or more continuous, three-dimensional Gaussian distance distributions. The method has previously been applied to studies of biological macromolecules[21–24], but has not been used for the analysis of RNA structure. In an initial application to nucleic acids, we showed that DNA four-way junctions exist as an equilibrium mixture of two conformational isomers[24].

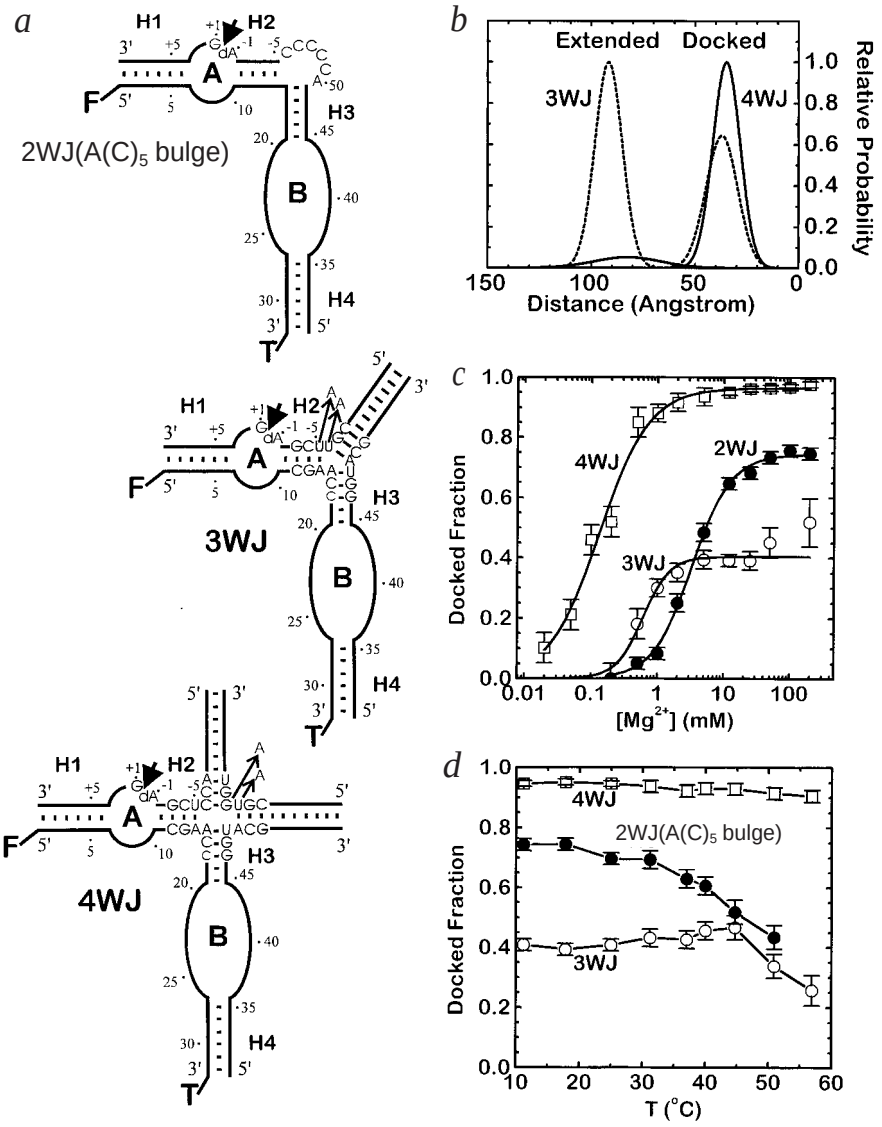

Fig. 2 Docking of modified junction designs of the hairpin ribozyme–substrate complex. ***a***, Ribozyme–substrate complexes with two- (2WJ), three- (3WJ), and four-way junctions (4WJ), respectively, as utilized in the present study. Only the sequence around the junction is shown. In the bulged version of the two-way junction, an $A(C)_5$ linker directly connects the substrate with the ribozyme. As an alternative to a fully base-paired, or perfect, helical junction, we introduced two mismatches into the three- and four-way constructs, as indicated by arrows. In all cases, the potential cleavage site (short arrow) is blocked by a 2′-deoxy modification of the attacking nucleophile of the A at position –1 with respect to the cleavage site. The positions of the fluorophores are indicated by F and T as in Fig. 1. ***b***, Distance distributions for the three-way (3WJ, dashed line) and four-way junction (4WJ, solid line) hairpin ribozyme–substrate complexes under standard conditions (12 mM $MgCl_2$, 17.8 °C). While the three-way junction docks to only 39% (mean end-to-end distance, 37 Å; full width at half-maximum probability (fwhm), 18 Å; $\chi^2 = 1.21$), the four-way junction favors docking, yielding 95% docked conformer (mean distance, 34 Å; fwhm, 15 Å; $\chi^2 = 1.27$). ***c***, Stability of tertiary structure folding, or docking, of different ribozyme–substrate complexes. Dependence of the docked fraction on Mg^{2+} concentration (at pH 7.5, 17.8 °C). Data were fitted with a cooperative binding equation to yield apparent dissociation constants for Mg^{2+} of 3.3 mM, 0.6 mM, and 0.1 mM and cooperativity coefficients of 1.5, 2.1, and 1.2 for the two-, three-, and four-way junction constructs, respectively. ***d***, Temperature dependence of the docked fraction of the two-, three-, and four-way junction constructs (at pH 7.5, 12 mM Mg^{2+}).

tr-FRET analysis of two-way junctions

Time-resolved FRET analysis of a G+1→A mutant hairpin ribozyme–substrate complex containing domain-terminal fluorophores (standard conditions: 50 mM Tris-HCl, pH 7.5, 12 mM Mg^{2+}, 17.8 °C) reveals a pattern of donor lifetimes indicative of a single interdomain distance distribution (Fig. 1*b*). The end-to-end distance distribution is centered around a mean distance of 77 Å, while the full width at half-maximum probability (fwhm, describing the width of the distribution) is 35 Å and reflects both fluorophore mobility and structural flexibility within the complex[21]. The mean distance is consistent with the overall length of an undocked, fully extended conformational isomer, which can be expected to display the equivalent of 32 stacked base pairs, with a rise of 2.3–2.9 Å per base pair[25]. Likewise, only undocked conformers were detected in the absence of substrate or when inhibitory mutations (for example, A40→G, U42→C, A43→G; Fig. 1*a*) were introduced into domain B (Table 1).

In sharp contrast, the analogous ribozyme–substrate complex containing the essential G+1 and a chemically blocking 2'-deoxy modification at the cleavage site (Fig. 1*a*) reveals a bimodal donor-acceptor distance distribution (Fig. 1*c*). 65% of the population is centered around a mean distance of 34 Å (fwhm, 18 Å), and 35% is centered around 78 Å (fwhm, 18 Å), respectively. The mean of the longer distance is essentially identical to that of the G+1→A mutant, suggesting similar extended global structures for both, while the majority of molecules have a much smaller end-to-end distance. We interpret the latter fraction as the docked, catalytically active conformer, in which the bend at the domain hinge brings the fluorophores into closer proximity (Fig. 1*c*). These results directly demonstrate that modification of the attacking nucleophile to 2'-deoxy or 2'-O-methyl (Table 1) does not interfere with docking, consistent with previous results[16,17]. It cannot be excluded that the inactive G+1→A mutant complex transiently accesses conformations with similar short end-to-end distances, but these lack specific interdomain interactions sufficient for significant population of a docked complex (Fig. 1*b*).

tr-FRET defines differences in RNA folding free energy

Application of tr-FRET to resolve and quantify the distribution between docked and extended complexes defines the equilibrium constant for docking (K_{dock} = docked fraction/extended

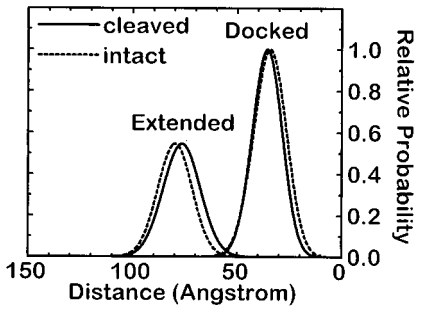

Fig. 3 Direct comparison of conformer distributions of the cleaved (solid line) and intact (dashed line) hairpin ribozyme–substrate complexes (based on 2WJ, Fig. 1*a*), under standard conditions (12 mM $MgCl_2$, 17.8 °C). The ternary complex between ribozyme and ligation substrate (or cleavage product) analogs yields 65% docked conformer with a mean end-to-end distance of 35 Å (fwhm, 17 Å; $\chi^2 = 1.34$), compared to 65% docked conformer for the complex in the presence of intact substrate (mean distance, 34 Å; fwhm, 18 Å; $\chi^2 = 1.28$). The structures of the extended conformers are also very similar, with mean distances of 75 Å (fwhm, 21 Å) and 78 Å (fwhm, 18 Å) for the cleaved and intact complexes, respectively.

fraction; Fig. 1*c*) and, hence, the associated free energy difference ($\Delta G_{dock} = -RT\ln(K_{dock})$) between two structurally defined minima in the folding free energy landscape of the hairpin ribozyme (Table 1). The extended complex appears to be stabilized by base stacking at the helical junction[26] (expected to be ~1–4 kcal mol^{-1}; ref. 27), while docking has to disrupt these stacks[13,16] and leads to specific interdomain contacts of similar stability; in fact, our measured values of ΔG_{dock} reflect the energetic difference between these two states. Analysis of the forces that favor one conformer over the other will lead to a deeper understanding of basic principles of RNA folding and to the design of more stably folded ribozymes for human gene therapy.

Modifying the interdomain junction

Our previous finding that the catalytic activity of the hairpin ribozyme may be influenced by modification of the interdomain junction[15] led to the hypothesis that the structure of the helical junction may be a key determinant in RNA folding as well. Accordingly, we conducted a systematic examination of the relationship between helical junction structure and the docking equilibrium. A50 is expected to compete with helix 2 for stacking onto helix 3 and thereby to destabilize the extended, inactive conformer[16] (Fig. 1*a*); indeed, deletion (Δ50) or mutation (U50) of this nucleotide shifts the equilibrium toward the extended form (Table 1). Linking the substrate to the ribozyme, through a bulge containing A followed by five C nucleotides ($A(C)_5$; Fig. 2*a*), stabilizes the docked conformer (Table 1), consistent with previous observations that bulges impose bends into RNA helical junctions[28]. Docking is destabilized under partially denaturing conditions (4 M urea; Table 1), indicating that the interdomain contacts are relatively weak, as previously suggested by domain separation experiments[13]. Constraining the linker to three, one, and no nucleotides progressively reduces the docked fraction to 26%, 21%, and <2%, respectively (Table 1), paralleling a decrease in activity[29]. These results establish tr-FRET as a valuable tool to analyze structural conformers of a biologically functional RNA.

Analysis of three- and four-way junctions (Fig. 2*a*; the latter found in the natural (-)-sTRSV RNA) shows that the configuration of the helical junction has a profound effect on formation of the active tertiary structure (Fig. 2*b*). In particular, the four-way junction strongly favors formation of the docked complex, leading to an equilibrium in which 95% of the molecules are docked (Table 1). Introducing two mismatches at the junction slightly reduces docking (to 93%) (Table 1), suggesting a role for pairwise coaxially stacked helices in docking of the four-way junction[20,21]. In contrast, a three-way junction was found to lead to only 39% docked complex (Fig. 2*b*, Table 1). In this case, additional flexibility at the junction by introducing two mismatched nucleotides increases docking to 43% (Table 1), paralleling an increase in catalytic activity[29].

The four-way junction strongly compensates for the loss of a specific loop A–loop B interaction; a G+1→A substitution or collapsing internal loops A and B into canonically base-paired helices still leads to 39% and 35% docking, respectively. In fact, 23% docked complex can even be detected in the absence of substrate (Table 1). Previously, substrate-independent tertiary structure formation could only be observed in footprinting experiments when Mg^{2+} ions were replaced by cobalt(III) hexammine, which appears to fold the ribozyme more stably than does magnesium[17]. While the structures of the four-way junctions with the G+1→A substitution, collapsed internal loops, or in the absence of substrate may slightly differ from that of the unmodified four-way junction, their global folds, as analyzed by tr-FRET, are indistinguishable.

These results are consistent with recent studies using comparative gel electrophoresis and steady-state FRET, indicating that the four-way junction can itself bring the arms carrying loops A and B into close physical proximity[20]. Our complementary time-resolved FRET measurements, however, emphasize that, without specific loop–loop interactions, a considerable fraction of complexes (61–65%) are in the form of the inactive, extended complex; specific interdomain interactions are necessary to shift the equilibrium toward the docked four-way junction complex. In the case of the less stably docked three-way junction hairpin ribozyme, eliminating specific interdomain contacts by a G+1→A substitution or by omission of substrate completely abolishes docking of the domains A and B (Table 1).

Influence of metal ions, temperature, and strand scission

Under physiological conditions (~1–2 mM Mg^{2+}), the relative enhancement of hairpin ribozyme folding by the four-way junction is still more dramatic. Here, the two-way junction yields the smallest fraction of docked complex (Fig. 2*c*). Its apparent K_D for Mg^{2+} in tertiary folding is 3.3 mM, *versus* 0.6 mM and 0.1 mM for the three-way and four-way junctions, respectively. These data do not exclude, however, that tight metal ion binding sites exist in the two- or three-way junction ribozymes that do not lead to domain docking as analyzed by tr-FRET.

What role do metal ions play in tertiary structure folding? When magnesium ions are replaced by low concentrations of sodium ions (100 mM), no docked two-way junction complexes can be detected. However, docking is partially restored by increasing Na^+ concentration to 2 M (Table 1), consistent with our observation of surprisingly efficient catalytic activity at high concentration of monovalent salts[30]. The finding that high concentrations of monovalent cations can substitute for divalent metal ions in both folding and catalysis supports a previously suggested model in which the key function of metal ions is to stabilize a catalytically proficient RNA structure, rather than to participate directly in reaction chemistry[13,30].

Analysis of the temperature dependence of docking shows that the four-way junction favors docking at significantly higher temperatures than does the two-way junction, although the docked conformer remains significantly populated for all constructs

Table 1 Equilibrium distribution between docked and extended conformers of hairpin ribozyme constructs with various modifications, as monitored by tr-FRET

Construct	modification[1]	Docked fraction (%)[2]	ΔG_{dock} (kcal mol^{-1})[3]
2WJ	S(G+1→A)	<2	>2.3
2WJ	no S	<2	>2.3
2WJ	Rz(A40→G, U42→C, A43→G)	<2	>2.3
2WJ	–	65 ± 2	-0.34 ± 0.03
2WJ	S(2′OMe A-1)	61 ± 2	-0.27 ± 0.06
2WJ	Rz(U50)	42 ± 2	+0.20 ± 0.03
2WJ	Rz(Δ50)	33 ± 2	+0.40 ± 0.06
2WJ(AC5 bulge)	–	74 ± 2	-0.62 ± 0.07
2WJ(AC5 bulge)	4 M urea	17 ± 2	+0.92 ± 0.08
2WJ(AC2 bulge)	–	26 ± 2	+0.60 ± 0.06
2WJ(A bulge)	–	21 ± 2	+0.76 ± 0.08
2WJ(no bulge)	–	< 2	> 2.3
3WJ	–	39 ± 2	+0.25 ± 0.04
3WJ	2 mismatches at junction	43 ± 2	+0.16 ± 0.05
3WJ	S(G+1→A)	< 2	> 2.3
3WJ	no S	< 2	> 2.3
4WJ	–	95 ± 1	-1.7 ± 0.1
4WJ	2 mismatches at junction	93 ± 1	-1.5 ± 0.1
4WJ	S(G+1→A)	39 ± 2	+0.26 ± 0.05
4WJ	base-paired loops A and B	35 ± 2	+0.37 ± 0.04
4WJ	no S	23 ± 2	+0.71 ± 0.06
2WJ	no Mg^{2+}, 100 mM Na^{+}	<2	>2.3
2WJ	no Mg^{2+}, 2 M Na^{+}	16 ± 2	+0.98 ± 0.07
2WJ	5'P+3'P	65 ± 2	-0.35 ± 0.04
2WJ	5'P(3'OH)+3'P	54 ± 2	-0.09 ± 0.04

[1]S = substrate, Rz = ribozyme, 5'P = 5'-product with 3'-phosphate, 5'P (3'OH) = 5-product with 3'-hydroxyl, 3'P = 3'-product; standard conditions were 1 μM fluorophore-labeled strand, 3 μM of each unlabeled strand (for product strands: 10 μM), in 50 mM Tris-HCl, pH 7.5, 12 mM $MgCl_2$, at 17.8 °C. If not stated otherwise, values are given for unmodified RNA sequences and standard conditions. [2]Docked and extended fractions together constitute 100% of the complexes; mean donor-acceptor distances were 31–38 Å (docked) and 65–100 Å (extended), with 15–30 Å and 15–50 Å fwhm, respectively. A value of <2 indicates the detection limit — that is, a good fit to the donor decay ($\chi^2 < 1.2$) was obtained with a single distance distribution corresponding to the extended conformer. [3]The free energy of docking ΔG_{dock} was calculated from $-RT\ln(K_{dock})$. The equilibrium constant K_{dock} is defined as indicated in Fig. 1*b* and was calculated from docked fraction/extended fraction. Errors were propagated from the estimate of typically 2% error in the docked fraction.

even at 50 °C. In each case, thermal disruption of the docked tertiary structure occurs gradually between 40 °C and 60 °C (Fig. 2*c*), paralleling an increase in UV absorption (data not shown). This property of the hairpin ribozyme resembles that of tRNA, where the tertiary structure and part of the secondary structure show overlapping melting transitions[31], and is distinct from melting of larger RNAs, such as group I ribozymes, where increasing temperature disrupts the tertiary structure before the secondary structure[32].

Ligation reactions are required for satellite RNA replication *in vivo*, and require assembly of a ternary complex for *trans* reactions *in vitro*. In the presence of saturating concentrations of ligation substrate analogs[16,17] (5'P and 3'P), the global structures of the extended and docked complexes and their equilibrium position are virtually identical to those observed with the cleavage substrate (Fig. 3, Table 1), indicating that the docked structure does not change significantly upon cleavage and that the energy differences between docked and extended complexes are the same for cleaved and intact substrates. Deletion of the 3'-phosphate group on the 5'-product analog, however, results in a small but significant shift away from the docked conformer (Table 1), consistent with the notion that the active site phosphate may function as a metal ion binding site to partially stabilize the docked complex.

Stable RNA folding in nature and gene therapy

In summary, our results indicate that the nature of the helical junction and of metal ion cofactors can shift the equilibrium distribution between docked and extended conformers from an undetectable (<2%) to a strongly prevalent (95%) docked fraction. ΔG_{dock} ranges between +2.3 and -1.7 kcal mol^{-1}, and can be measured by tr-FRET with high precision. The global structures of both the docked and extended conformer, as observed by tr-FRET with near Å resolution of their end-to-end distances, are virtually unchanged among all hairpin ribozyme–substrate complexes and are clearly separable from one another.

RNA two-, three-, and four-way junctions are ubiquitous elements of RNA secondary structure. By introducing tr-FRET as a tool to study a ribozyme containing these junctions, we are able to quantitatively compare their impact on the stability of a biologically active tertiary structure. What do we learn from these studies? First, we begin to understand the thermodynamics of a catalytic RNA folding free energy landscape. Second, the measured intramolecular distances can be used as a constraint in molecular modeling of the active structure. Third, and most important, our results indicate that nature may have optimized hairpin ribozyme folding at physiological Mg^{2+} concentrations by virtue of a four-way helical junction. Our results directly demonstrate that a perfect four-way junction, as found in (-)-sTRSV RNA, dramatically stabilizes the docked and catalytically active conformer; it appears to be nature's choice as a scaffold to favor docking of distant domains of an RNA molecule, provided that additional, specific RNA–RNA interactions between the domains exist. In contrast, natural RNA three-way junctions, that need to dock into an analogous wishbone shape for their biological function, appear to require either extensive bulges at their junctions (as in the hammerhead ribozyme[18,33]), or the binding of a protein cofactor (as in the S15 binding site of 16S rRNA[34]) to bring two of their three arms into proximity. These observations are consistent with our finding of unstable docking of a perfect three-way junction hairpin ribozyme. Incorporation of a bulge or binding of a protein cofactor at this three-way junction could overcome the modest (1–2 kcal mol^{-1}), but crucial energetic barrier for shifting the equilibrium toward an active docked conformer. Since human gene therapy utilizes ribozymes to target undesired intracellular RNAs, these results have immediate implications for the design of RNAs that need to fold stably and in a controllable fashion under physiological conditions.

Methods

Preparation of RNA samples. All RNA was synthesized on an Applied Biosystems 392 DNA/RNA synthesizer, using standard solid-phase phosphoramidite chemistry, with reagents supplied by Glen Research. Sequences were: for the 5′-fluorescein (F) and 3′-tetram-

ethylrhodamine (T) labeled ribozyme strand, 5′-F-AAAUAGAGAAGCGAACCA-GAGAAACACACGCC-T-3′; in addition, for 2WJ, 5′-GGCGUGGUACAUUACCUGGUA-3′ and 5′-UCGCdAGUCCUAUUU-3′; for 2WJ(AC_5 bulge), 5′-GGCGUGGUACAUUACCUGGUACCCCC-UCGCdAGUCCUAUUU-3′; for 3WJ, 5′-GGCGUGGUACAUUACCUGGUACGAGUUGAC-3′ and 5′-GUCAACUCGUUCGCdAGUCCUAUUU-3′; and for 4WJ, 5′-GGCGUGGUACAUUACCUGGU-ACGAGUUGAC-3′, 5′-GUCAACUCGUGGUGGCUUGC-3′, and 5′-GCAAGCCACCUCGCdAGUCCUAUUU-3′. 5′-fluorescein was coupled during synthesis. The FRET acceptor (tetramethylrhodamine) was attached post-synthetically, utilizing an incorporated 3′-amino-modifier C7. Oligonucleotides were purified by denaturing 20% polyacrylamide gel electrophoresis, diffusion elution from the gel slices, ethanol precipitation, and C_8-reverse-phase HPLC chromatography in 100 mM triethylammonium acetate, with a linear elution gradient of 0–60% acetonitrile (50 min, 1 ml min^{-1}). Tetramethylrhodamine was reacted as a succinimidyl ester (Molecular Probes) with the 3′-amino-modifier, and the doubly-labeled oligonucleotide was again ethanol precipitated and HPLC purified. All RNA complexes were prepared in standard cleavage buffer (50 mM Tris-HCl, pH 7.5, 12 mM $MgCl_2$), if not stated otherwise, with the fluorophore-labeled strand in 1 μM concentration and all other strands in a saturating three-fold excess (10-fold in case of the cleavage product analogs). Higher concentrations of the unlabeled strands did not lead to any changes in the observed fluorescence signals. The mixture was heat-denatured for 2 min at 70 °C, then allowed to cool to room temperature over 5 min.

Fluorescence measurements. The sample (150 μl) was incubated in a quartz cuvette at measurement temperature (standard: 17.8 °C) for at least 15 min, prior to collecting time-resolved emission profiles of the fluorescein donor using time-correlated single photon counting as described[21]. Pulsed excitation was at 514 nm, isotropic emission detection to >40,000 peak counts under magic angle conditions at 530 nm (16 nm slit width plus 530 nm cut-off filter). Decays were collected in 2,048 channels with a sampling time of 18.0 ps per channel.

Data analysis. To derive distance information, two time-resolved fluorescence decays were collected, one for the sample with acceptor in place, one under identical conditions but employing a donor-only RNA complex. The decay of fluorescein emission in the doubly-labeled complex was analyzed by a model of distance distributions[24]

$$I_{DA}(t) = \sum_k f_k \int P_k(R) \sum_i \alpha_i \exp\left[-\frac{t}{\tau_i}\left(1+\left(\frac{R_0}{R}\right)^6\right)\right] dR \quad (1)$$

where the first sum refers to the number of distributions, either one or two, each with fractional population f_k and distance distribution $P_k(R)$. The distribution was modeled as a weighted Gaussian,

$$P(R) = 4\pi R^2 c \exp\left[-a(R-b)^2\right] \quad (2)$$

where *a* and *b* are parameters that describe the shape of the distribution and c is a normalization constant. Equation 1 was used to fit experimental data by non-linear least squares regression, with a, b, and f_k for each distribution as adjustable parameters. Two distance distributions were used for analysis when a single distribution failed to give a good fit, as judged by the reduced χ^2 value and by inspection of residuals. In all such cases the inclusion of a second distribution resulted in a dramatic improvement of the fit. The intrinsic donor lifetimes τ_i and decay amplitudes α_i were determined for each set of experimental conditions by a sum-of-exponentials fit to the donor intensity decay in the donor-only molecule. The Förster distance R_0 was evaluated for the donor-acceptor pair (R_0 = 55 Å) according to standard procedures[21] and assuming a value of 2/3 for the orientation factor. The latter assumption is supported by time-resolved fluorescence anisotropy decay experiments, performed as described[21], which reveal large amplitude rotational motions of both fluorescein and tetramethylrhodamine, characterized by half cone angles of 28° and 42°, respectively.

The dependence of the docked fraction on the Mg^{2+} concentration was fitted to the cooperative binding equation

$$f = f_{\max} \frac{[Mg^{2+}]^n}{[Mg^{2+}]^n + (K_D^{Mg})^n} \quad (3)$$

as described[16,17] to yield an apparent dissociation constant K_D^{Mg} for Mg^{2+} and a cooperativity coefficient n.

Acknowledgments

We thank W. Lam and E. Thompson for help in setting up the laser system and data analysis and D. Pecchia for RNA synthesis. This work was supported by grants from the National Institutes of Health in the USA and an Otto-Hahn medal fellowship from the Max-Planck Society for NGW.

Correspondence should be addressed to D.P.M. *e-mail: millar@scripps.edu*

Received 19 October, 1998; accepted 12 February, 1999.

1. Kruger, K. *et al. Cell* **31**, 147–157 (1982).
2. Guerrier-Takada, C., Gardiner, K., Marsh, T., Pace, N. & Altman, S. *Cell* **35**, 849–857 (1983).
3. Conn, G.L. & Draper, D.E. *Curr. Opin. Struct. Biol.* **8**, 278–285 (1998).
4. Bevilacqua, P.C., Kierzek, R., Johnson, K.A. & Turner, D.H. *Science* **258**, 1355–1358 (1992).
5. Narlikar, G.J. & Herschlag, D. *Nature Struct. Biol.* **3**, 701–710 (1996).
6. Pan, T. & Sosnick, T.R. *Nature Struct. Biol.* **4**, 931–938 (1997).
7. Pan, J., Thirumalai, D. & Woodson, S.A. *J. Mol. Biol.* **273**, 7–13 (1997).
8. Sclavi, B., Sullivan, M., Chance, M.R., Brenowitz, M. & Woodson, S.A. *Science* **279**, 1940–1943 (1998).
9. Treiber, D.K., Rook, M.S., Zarrinkar, P.P. & Williamson, J.R. *Science* **279**, 1943–1946 (1998).
10. Buzayan, J.M., Gerlach, W.L. & Bruening, G. *Nature* **323**, 349–353 (1986).
11. Hampel, A. & Tritz, R. *Biochemistry* **28**, 4929–4933 (1989).
12. Earnshaw, D.J. & Gait, M.J. *Antisense Nucleic Drug Dev.* **7**, 403–411 (1997).
13. Walter, N.G. & Burke, J.M. *Curr. Opin. Chem. Biol.* **2**, 24–30 (1998).
14. Esteban, J.A., Banerjee, A.R. & Burke, J. M. *J. Biol. Chem.*, **272**, 13629–13639 (1997).
15. Esteban, J.A., Walter, N.G., Kotzorek, G., Heckman, J.E. & Burke, J.M. *Proc. Natl. Acad. Sci. USA* **95**, 6091–6096 (1998).
16. Walter, N.G., Hampel, K.J., Brown, K.M. & Burke, J.M. *EMBO J.* **17**, 2378–2391 (1998).
17. Hampel, K.J., Walter, N.G. & Burke, J.M. *Biochemistry* **37**, 14672–14682 (1998).
18. Tuschl, T., Gohlke, C., Jovin, T.M., Westhof, E. & Eckstein, F. *Science* **266**, 785–789 (1994).
19. Murchie, A.I.H., Thomson, J.B., Walter, F. & Lilley, D.M.J. *Mol. Cell* **1**, 873–881 (1998).
20. Walter, F., Murchie, A.I.H., Duckett, D.R. & Lilley, D.M.J. *RNA* **4**, 719–728 (1998).
21. Eis, P.S. & Millar, D.P. *Biochemistry* **32**, 13852–13860 (1993).
22. Wu, P.G., James, E. & Brand, L. *Biophys. Chem.* **48**, 123–133 (1993).
23. Ittah, V. & Haas, E. *Biochemistry* **34**, 4493–4506 (1995).
24. Miick, S.M., Fee, R.S., Millar, D.P. & Chazin, W.J. *Proc. Natl. Acad. Sci. USA* **94**, 9080–9084 (1997).
25. Saenger, W. *Principles of Nucleic Acid Structure*. (Springer Press, Berlin; 1984).
26. Walter, N.G. & Burke, J.M. *RNA* **3**, 392–404 (1997).
27. Walter, A.E. *et al. Proc. Natl. Acad. Sci. USA* **91**, 9218–9222 (1994).
28. Zacharias, M. & Hagerman, P.J. *J. Mol. Biol.* **247**, 486–500 (1995).
29. Komatsu, Y., Shirai, M., Yamashita, S. & Ohtsuka, E. *Bioorg. Med. Chem.* **5**, 1063–1069 (1997).
30. Murray, J.B., Seyhan, A.A., Walter, N.G., Burke, J.M. & Scott, W.G. *Chem. Biol.* **5**, 587–595 (1998).
31. Johnston, P.D. & Redfield, A.G. *Biochemistry* **20**, 3996–4006 (1981).
32. Banerjee, A.R., Jaeger, J.A. & Turner, D.H. *Biochemistry* **32**, 153–163 (1993).
33. Wedekind, J.E. & McKay, D.B. *Annu. Rev. Biophys. Biomol. Struct.* **27**, 475–502 (1998).
34. Batey, R.T. & Williamson, J. R. *RNA* **4**, 984–897 (1998).